

A Two Variable Experimental Study in Rectangular Open Channels of Smooth Boundaries

John Demetriou¹, Eugene Retsinis², Gerassimos Ballas³
^{1,2,3} Civil Engineer, National Technical University of Athens (NTUA), Greece

Abstract: In this experimental study a two variable investigation of pertinent velocity laboratory measurements is presented, analyzed and discussed. The research deals with the uniform-steady-turbulent water flows within an almost horizontal, smooth, rectangular open channel. The local (point) velocities were electronically measured in two long channels with low and medium-low aspect ratios (groups A, B), and a third channel with high aspect ratios (group C). The hydraulic centre's (H.C.) position on the vertical axis of symmetry is examined, after measuring a very large number of local velocities. A number of velocity diagrams in $Y=y/0.5 \cdot b$ and $Z=z/z_n$ (cross sections $b \cdot z_n$, y , z , axes) coordinates are also presented. A diagram of vertical strips within all water cross sections is created, and the internal distribution of partial discharges is examined in dimensionless terms. All dimensionless velocities \bar{U} are considered as two variable functions of Y and Z , $\bar{U}=f(Y, Z)$, and all data are elaborated with the aid of a computer program, giving a number of computer isovelocity lines, $\bar{U}=\text{const}$. A number of equations are also proposed in order to better examine the flows' structures, aiming on helping the hydraulic engineer when analyzing the mechanism of flow.

Keywords: Open Channels, Smooth Boundaries, Velocities' Two Variable Analysis.

I. Introduction

One of the basic uniform-steady-turbulent flows in open channel hydraulics is the smooth boundary case-within a rectangular cross section (Fig. 1). The structure of the velocity field of this water flow, although the extensive research in the past, still is of considerable interest.

At any point y, z , with $0 \leq y \leq 0.5 \cdot b$ and $0 \leq z \leq z_n \leq H$ of the semi-cross section ($0.5 \cdot b \cdot z_n$) the turbulent mean time x velocity is \bar{u} (or in dimensionless terms $\bar{U}=\bar{u}/V$), where with the water discharge (Q) the average cross sectional velocity is $V=Q/E$. On the flow axis (centre line plane) $y=0.5 \cdot b$, the maximum local velocity is \bar{U}_{max} (at a height $z=z_m$ -Hydraulic Centre), the longitudinal channel slope $J_0=\sin\phi$ -usually is very small (of the order of 0.001-0.0023), while the aspect ratio of the entire semi cross section is $\lambda=2 \cdot z_n/b$.

A very well known characteristic of this flow is that the flow stream lines are not exactly straight lines but helicoidal lines, since they are distorted from the secondary turbulent flow field, v', w' , where $v=\bar{v}+v'$ and $w=\bar{w}+w'$. Thus, the final result is that on any water cross section a number of weak closed vortices are formed. Sometimes it is useful to work with the depth-mean velocities along a vertical line (or strip)

$$\bar{u} = (1/z_n) \cdot \int_0^{z_n} \bar{u} dz, \text{ or, } \bar{U} = \bar{u}/V = (1/z_n) \cdot \int_0^{z_n} (\bar{u}/V) dz,$$

several results of which will be shown in this research.

In the present experimental investigation the local dimensionless velocities $\bar{U}=\bar{u}/V$ are mainly measured in a rectangular channel of smooth boundaries as two variable functions of both $y/0.5 \cdot b$ and z/z_n ,

$$\bar{U}=\bar{u}/V=f(y/0.5 \cdot b, z/z_n),$$

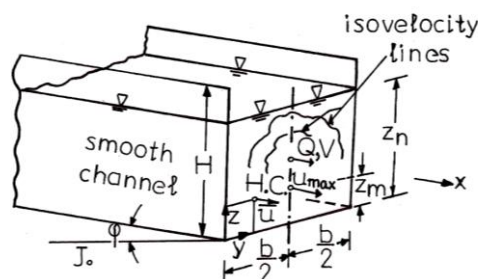


Figure 1. Geometry of flow.

and some of them are treated with the aid of computational methods. The final results are equations for various discharges and coordinates and a number of diagrams concerning the isovelocity lines $\bar{U}=\text{const}$., given by the computer.

From the older data, the pertinent issues by Chow (1959), [1], Goncharov (1964), [2] (who has investigated the H.C.) and Knight et al (1982), [3], are chosen as important here, while of some interest could be the paper by Demetriou, (1983), [4], and the book by the same author, (2008), [5]. Moreover, in the paper by

Knight et al (1983), [6], some interesting details on the experimental processes may be found.

It is to be noted that the concepts of smooth boundaries and hydraulically smooth channels are greatly differing between them.

II. Experiments

Three rigs were used in this investigation: (i) Groups' A data were undertaken in a long smooth (perspex) channel ($l \approx 15$ m), with $b=15.2$ cm. (ii) Groups' B measurements were performed in a long smooth (perspex) channel ($l \approx 12$ m), with $b=25$ cm, while, (iii) Groups' C measurements were undertaken in a shorter smooth channel with $b=10$ cm. The various laboratory elements are given in Table 1, where all discharges Q were measured by corresponding Venturi meters and suitable manometers, following proper electric pumps.

All A and C measurements' series were performed in the hydraulics laboratory of the Univ. of Birmingham (UK), while B series measurements were undertaken in the hydraulics laboratory of the Univ. of Athens (NTUA)-Greece.

In all laboratory series a number of about 1,000 local (point) velocities (\bar{u}) were measured, with the aid of a Pitot tube (external diameter 3.4 mm-B series), or an industrial miniature electronic propeller (A, C, series) supplied with revolving blades (of 4 mm size). This instrument could reliably measure velocities at minimum distances from any solid or water boundaries, at around 7.5 mm. In any turn of the blades the electric impedance was measured (in Hz) and corresponding velocity \bar{u} was determined through a pre-fabricated linear chart (Hz- \bar{u}). The flow's uniformity was succeeded through a suitable tail gate (Groups A, B), or another proper solid hydraulic construction within the downstream flow (Group C).

Table 1. Laboratory Elements

Group A						Group B					
N ^o	Q cm ³ /sec	z _n cm	V cm/sec	z _m /z _n	λ	N ^o	Q cm ³ /sec	z _n cm	V cm/sec	z _m /z _n	λ
A ₁	4,800	8.44	37.41	0.59	1.11	B ₁	7,400	7.44	37.98	0.85	0.59
A ₂	5,600	9.50	38.78	0.55	1.25	B ₂	7,440	8.62	34.52	0.81	0.69
A ₃	6,070	10.13	39.42	0.69	1.33	B ₃	9,010	9.27	38.88	0.85	0.74
A ₄	7,000	11.40	40.39	0.61	1.50	B ₄	9,600	11.05	34.75	0.73	0.88
A ₅	8,000	12.67	41.51	0.55	1.67	B ₅	10,170	11.65	34.01	0.86	0.93
A ₆	9,850	15.20	42.63	0.59	2.00	B ₆	17,610	15.21	46.31	0.77	1.22
A ₇	11,820	17.60	44.18	0.56	2.32	B ₇	10,150	15.94	50.73	0.76	1.28
Group C						B ₈	24,530	18.83	52.11	0.84	1.51
C ₁	3,627	21.3	17.03	0.65	4.26	B ₉	27,170	19.71	54.97	0.83	1.58
C ₂	5,510	23.45	23.50	0.63	4.69	B ₁₀	28,106	21.32	52.72	0.76	1.71
C ₃	7,792	25.91	30.07	0.61	5.18	B ₁₁	30,860	22.57	54.69	0.77	1.81
C ₄	10,288	28.55	36.04	0.62	5.71						

Following \bar{u} measurements, the $\bar{u}/V=\bar{U}$ ratios against $y/0.5 \cdot b=Y$ and $z/z_n=Z$ dimensionless coordinates were determined, and a large number of \bar{U} (against Y -at any $Z=\text{const.}$) graphical diagrams were constructed.

Finally, all water semi-cross sections of A₁ to A₆ groups of measurements were divided by suitable vertical lines in water strips of constant widths $\Delta(y/0.5 \cdot b)=0.05$, and the corresponding depth-mean velocities \bar{u} were determined in terms of $\bar{U}=\bar{u}/V$, giving-after a proper smoothing out-a unique \bar{U} value vs $Y=y/0.5 \cdot b$ diagram, holding for all present velocities' measurements. The last elaboration may give the experimental internal distribution of all particular discharges Q_i -especially in Q_i/Q terms, in those water strips, i.e. it may give the experimental composition of Q_i/Q within the entire semi-cross sections, for all present measurements.

III. Results/Analysis

Fig. 2 presents z_m/z_n ratios on the centerline flow axes vs λ , for all present Groups. On this Figure, from Group B (low λ , high z_m/z_n), a proper curve was traced through Group A (medium λ and z_m/z_n) to Group C (high λ , and medium z_m/z_n). In Group B z_m/z_n curve is abruptly falling, while through Group A the curve is slowly rising again (two Group C).

The above behavior is in general agreement with Goncharov's, (1964), [2], results and actually shows the end of the boundary layer on the central plain along the flow.

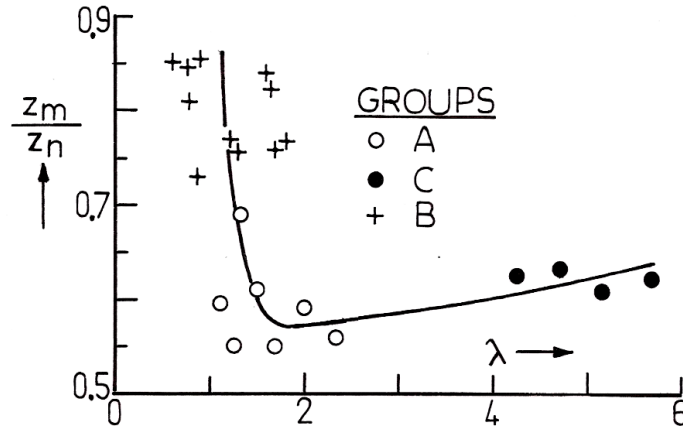


Figure 2. z_m/z_n vs λ for Groups.

Figs. 3 and 4 present some preliminary experimental results concerning \bar{U} vs $Y=y/0.5 \cdot b$ and $Z=z/z_n$, for two typical series A_1 and A_5 . As it may be seen all velocities are normally varying along Y , and thus these curves could be extrapolated to-corresponding free water surfaces and to zero values (on the beds).

Fig. 5 shows all $\bar{U}=\bar{u}/V$ distributions along Y , where \bar{u} are depth-mean velocities along a number of equal vertical strips with widths $\Delta(y/0.5 \cdot b)=0.05$. The discharge in each strip is the corresponding \bar{U} multiplied by 0.05 and expressed as a percentage. This result (%) on the i strip represents $0.5 \cdot Q_i / 0.5 \cdot Q$ where $0.5 \cdot Q_i$ is the water discharge in the i strip and $0.5 \cdot Q$ is the total discharge over the semi-cross section. This diagram holds for all present laboratory results of Group A, and shows the experimental internal distribution of all partial discharges of this study, i.e. 3.95%, 4.35%,... All these $0.5 \cdot Q_i$ percentages give a summation of $\approx 100\%$ in the semi-cross section. Perhaps this discharge has a wider interest for all smooth rectangular open channels of A Group.

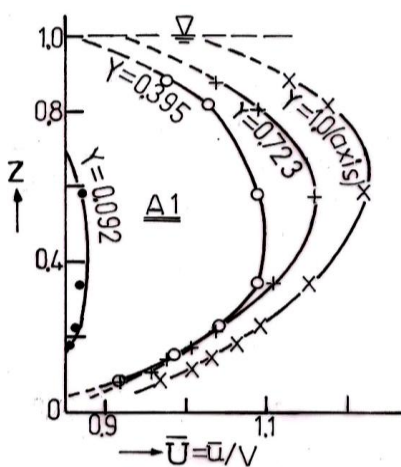


Figure 3. \bar{U} vs Y and Z for A_1 .

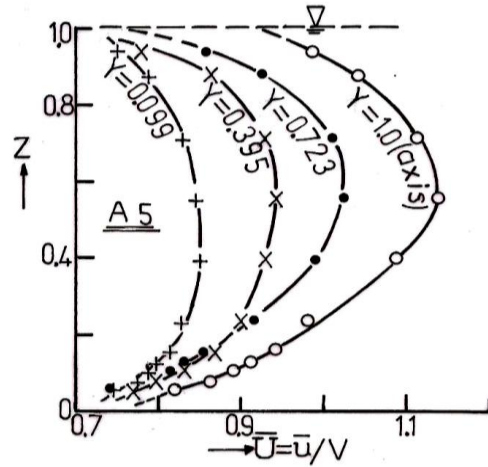


Figure 4. \bar{U} vs Y and Z for A_5 .

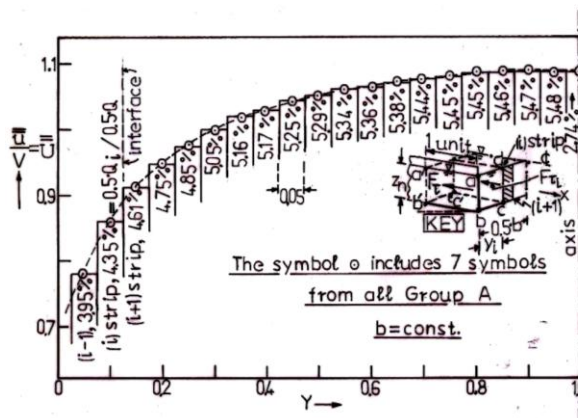


Figure 5. Discharge distribution in semi-cross section.

In Fig. 5 (KEY) suppose that the water control volume (c.v.) of unit length along x, (abcd) = z_n·y_i·1, where ab=cd=a'b'=z_n, while (z_n·1) is also the internal (imaginary) left side surface of the (i) vertical strip. Since the flow is uniform, in both (z_n·y_i) front and rear surfaces, the hydrostatic pressures are the same, i.e. F_{p_x}=0. Along the part of the solid boundary, (z_n+y_i)·1, the boundary shear force F_τ is opposing the flow, while on z_n·1-left surface of the strip (i), the corresponding shear force (apparent shear force) is F_{τ_i}. If, on the above c.v., the x momentum equation is applied, then F_τ+F_{τ_i}=(water weight component)=(z_n·y_i)·ρ·g·J_o·1=F_g, or F_{τ_i}=[F_g-F_τ]. Thus, the apparent shear force may be calculated if F_g and F_τ are known. It is easy to determine F_g, while F_τ may result either: (1). If the local (point) shear stresses are experimentally determined on surfaces (z_n+y_i)·1, followed by an integration of them along these surfaces, or, (2). If τ_{om} is the well known mean boundary shear stress (as in any open channel uniform flow), F_τ=τ_{om}·(z_n+y_i)·1. On the other hand it is well known that, τ_{om}=ρ·g·R·J_o, where R is the hydraulic radius R=(0.5·b·λ)·(1+λ)⁻¹, and thus

$$F_{\tau} = 0.125 \cdot \rho \cdot g \cdot J_o \cdot b^2 \cdot (\lambda + Y_i) \cdot (\lambda + 1)^{-1},$$

becoming max when Y_i=1 and increasing with J_o, level of turbulence and wall's roughness. A similar analysis holds for horizontal layers.

The above mechanism explains the water momentum transfer from centre line vertical plane to the walls (and to free surface and channel bed). It is responsible for the \bar{U} variation perpendicularly to the flow, and consequently for the \bar{U} change along Y or Z (Fig. 5), Knight et al (1982), [3], (1983), [6], and Demetriou, (2008), [5].

Table 2 indicatively presents all measured values $\bar{u}/V = \bar{U}$ vs Y and Z dimensionless coordinates in the function $\bar{U} = f(Y, Z)$, for two characteristic flows (A₂ and A₃) in the channel, where all \bar{U} values on the solid boundaries ($\bar{U}=0$) or on the free water surfaces were also taken into consideration.

Table 2. Measured and Predicted \bar{U} .

$\bar{U} = f(Y, Z)$									
A ₂ , r ² ≈0.92					A ₃ , r ² ≈0.92				
N ^o	Y Value	Z Value	\bar{U} Value	\bar{U} Predict	N ^o	Y Value	Z Value	\bar{U} Value	\bar{U} Predict
1	1	0	0	-	1	1	0	0	-
2	1	0.079	0.890	0.8250955	2	1	0.074	0.863	0.8006453
3	1	0.105	0.896	0.9170852	3	1	0.099	0.883	0.8954812
4	1	0.137	0.946	0.986896	4	1	0.128	0.921	0.9667821
5	1	0.168	0.962	1.0207285	5	1	0.158	0.939	1.007204
6	1	0.210	0.985	1.0317461	6	1	0.197	0.969	1.024685
7	1	0.263	1.021	1.0162621	7	1	0.247	1.005	1.0141294
8	1	0.316	1.047	0.9936951	8	1	0.296	1.035	0.9912943
9	1	0.526	1.135	1.0302155	9	1	0.494	1.116	0.9999867
10	1	0.734	1.106	1.0720519	10	1	0.691	1.126	1.0967345
11	1	0.916	1.037	0.9232934	11	1	0.888	1.055	0.9638362
12	1	1.000	1.037	-	12	1	0.947	0.994	0.9268352
13	0.724	0	0	-	13	1	1	0.994	-
14	0.724	0.079	0.879	0.8243455	14	0.724	0	0	-
15	0.724	0.105	0.921	0.9163352	15	0.724	0.074	0.877	0.8065683
16	0.724	0.137	0.949	0.986146	16	0.724	0.099	0.913	0.9014043
17	0.724	0.168	0.97	1.0199785	17	0.724	0.128	0.936	0.9727052
18	0.724	0.210	1.000	1.0309961	18	0.724	0.158	0.984	1.0131271
19	0.724	0.263	1.044	1.0155121	19	0.724	0.197	0.994	1.0306081
20	0.724	0.316	1.075	0.9929451	20	0.724	0.247	1.020	1.0200525
21	0.724	0.526	1.134	1.0294655	21	0.724	0.296	1.053	0.9972173
22	0.724	0.734	1.101	1.0713019	22	0.724	0.494	1.129	1.0059097
23	0.724	0.926	0.990	0.9225434	23	0.724	0.691	1.121	1.1026576
24	0.724	1.000	0.990	-	24	0.724	0.888	1.032	0.9697593
25	0.395	0	0	-	25	0.724	0.946	0.959	0.9327582
26	0.395	0.079	0.895	0.8079288	26	0.724	1	0.959	-
27	0.395	0.105	0.931	0.8999185	27	0.395	0	0	-
28	0.395	0.137	0.959	0.9697293	28	0.395	0.074	0.893	0.7863376
29	0.395	0.168	0.980	1.0035619	29	0.395	0.099	0.928	0.8811735

30	0.395	0.210	1.016	1.0145794	30	0.395	0.128	0.961	0.9524744
31	0.395	0.263	1.044	0.9990955	31	0.395	0.158	0.984	0.9928963
32	0.395	0.316	1.052	0.9765285	32	0.395	0.197	1.012	1.0103774
33	0.395	0.526	1.070	1.0130488	33	0.395	0.247	1.027	0.9998217
34	0.395	0.734	1.037	1.0548852	34	0.395	0.296	1.040	0.9769866
35	0.395	0.926	0.936	0.9061267	35	0.395	0.494	1.071	0.985679
36	0.395	1.000	0.936	-	36	0.395	0.691	1.045	1.0824268
37	0.092	0	0	-	37	0.395	0.888	0.967	0.9495285
38	0.092	0.079	0.786	0.6582621	38	0.395	0.946	0.893	0.9125275
39	0.092	0.105	0.905	0.7502519	39	0.395	1	0.893	-
40	0.092	0.137	0.817	0.8200626	40	0.092	0	0	-
41	0.092	0.168	0.830	0.8538952	41	0.092	0.074	0.781	0.6315683
42	0.092	0.210	0.841	0.8649128	42	0.092	0.099	0.789	0.7264043
43	0.092	0.263	0.851	0.8494288	43	0.092	0.128	0.807	0.7977052
44	0.092	0.316	0.854	0.8268618	44	0.092	0.158	0.819	0.8381271
45	0.092	0.526	0.848	0.8633822	45	0.092	0.197	0.835	0.8556081
46	0.092	0.734	0.812	0.9052185	46	0.092	0.247	0.845	0.8450525
47	0.092	0.943	0.758	0.75646	47	0.092	0.296	0.842	0.8222173
48	0.092	1.000	0.758	-	48	0.092	0.494	0.852	0.8309097
					49	0.092	0.691	0.835	0.9276576
					50	0.092	0.888	0.791	0.7947593
					51	0.092	0.946	0.753	0.7577582
					52	0.092	1	0.753	-

Based on the measured values of all six first flows (A) eqs. (1) to (6) were provided by the computer program, and the predicted, by those equations, \bar{U} values were also determined. For the two flows of Table 2 it is remarkable that measured and predicted \bar{U} values are very close among them (the majority of differences are of the order of $\approx \pm 10\%$). This happens for all the rest of the flows, being essential in order that the computer model predicted from all flows' equations is correct.

Based on all A measurements' results the following equations (1)-(6)-of the same type-are produced for all cross sections,

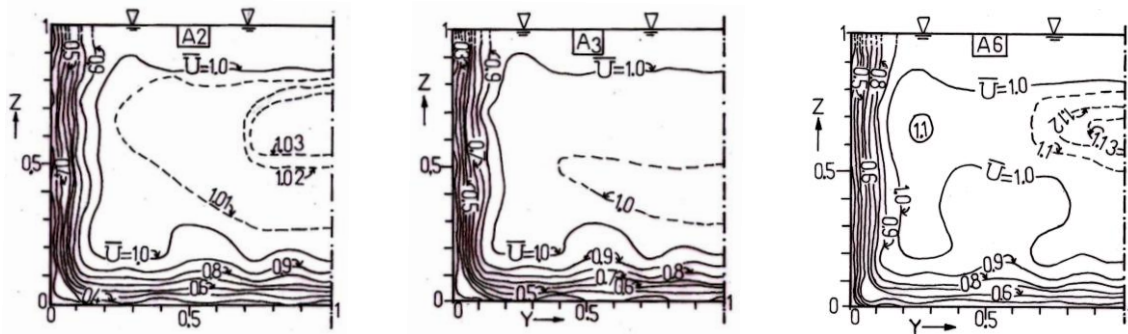
$$\bar{U}_i = (a_i) + (b_i) \cdot Y + (c_i) \cdot Y^2 + (d_i) \cdot Y^3 + (e_i) \cdot Y^4 + (f_i) \cdot Z + (g_i) \cdot Z^2 + (h_i) \cdot Z^3 + (k_i) \cdot Z^4 + (j_i) \cdot Z^5, \quad (1)-(6)$$

where $i=1, 2, 3, 4, 5, 6$. All pertinent arithmetic coefficients' values $a_i, b_i, c_i, d_i, e_i, f_i, g_i, h_i, k_i, j_i$ are shown in Table 3.

Table 3. Arithmetic Coefficients' Values for Eqs. (1) to (6).

	a_i	b_i	c_i	d_i	e_i	f_i	g_i	h_i	k_i	j_i	Remarks	
$i=1$	-0.680	12.010	-44.149	60.044	-26.985	9.945	-45.615	96.056	-92.890	33.251	For all cross sections (A ₁ -A ₆).	
$i=2$	-0.667	11.614	-42.031	56.650	-25.311	10.805	-54.228	120.296	-	119.780		43.641
$i=3$	-0.656	11.470	-41.420	55.831	-24.966	10.677	-53.429	117.290	-	114.896		41.052
$i=4$	-0.631	11.234	-40.634	54.862	-24.559	10.671	55.287	125.332	-	126.446		46.423
$i=5$	-0.622	10.719	-37.989	50.807	-22.628	10.727	-54.614	121.356	-	120.180		43.378
$i=6$	-0.578	11.162	-40.327	54.419	-24.343	10.138	-53.027	120.778	-	122.012		44.745

Fig. 6 shows diagrams of isovels $\bar{U}=f(Y, Z)=\text{const.}$ for all present measurements (A₂, A₃, A₆), given by the computer (continuous lines) and supplemented by secondary results (dashed lines).

Figure 6. $\bar{U}=\text{const.}$ (isovels) for A_2, A_3, A_6 flows.

As one can see from Fig. 6, the results cover almost all flow fields of the three A series. The dense isovels close to the solid walls and beds show the boundary layers created, while all curves terminate perpendicularly to corresponding flow axes.

The detailed velocity measurements for the C series of measurements are not shown here (although elaborated in the same way) two isovelocity lines' data are further presented, in order to show the results for high λ , C series-Fig. 7, where the dashed curves are the results of interpolations.

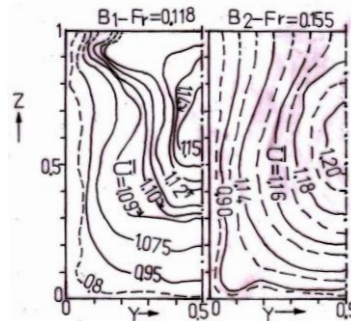


Figure 7. Isovels for Group B

IV. Conclusions

In this experimental and computational study a two variable investigation of the velocity field in uniform-steady-turbulent flows within a horizontal smooth boundaries' rectangular open channel is presented-analyzed and discussed. The main conclusions are: 1). The hydraulic centre (H.C.) depends on the form of water semi cross sections (low, medium or high), i.e. on the aspect ratio λ . 2). Fig. 2 shows that high λ values correspond to ascending positions of H.C., while low λ values correspond to dimensionless coordinates). 4). Fig. 5 presents all dimensionless velocity measurements (\bar{U}) as functions of Y. 5). In the previous Figure the internal distribution of the partial discharges within the general semi-cross section is investigated. 6). An explanation is provided on the role of the apparent shear forces within all cross sections. 7). In Table 2 a large number of local velocities (\bar{U}) are given for two typical groups of A flows. 8). A number of equations are given for the dimensionless velocities, \bar{U} , as two variable functions of Y and Z, which were also provided by a suitable computer program. 9). A number of isovelocity curves $\bar{U}=\text{const.}$ are given (by the computer) in order to better realise the flow structure. The present investigation is aiming at assisting the hydraulic engineer when analyzing the mechanism of such flows.descending positions of H.C. 3). Figs. 3 and 4 present a number of dimensionless velocities \bar{U} as functions of Y, Z (horizontal and vertical

References

- [1] V. T. Chow, *Open Channel Hydraulics* (Mc Graw-Hill Book Co., New York, pp. 24-25, 1959).
- [2] V. Goncharov, *Dynamics of Channel Flow* (Translated from Russian, Israel Program for Scientific Translations, Jerusalem, 1964).
- [3] D. W. Knight, H. S. Patel, J. D. Demetriou and M. E. Hame, Boundary Shear Stress Distributions in Open Channel and Closed Conduit Flows, *Enromech 156, Istanbul, Turkey, 1982, 6 pages.*
- [4] J. Demetriou, A Simple Method to Measure Shear Stresses in Open Channels, *Journal of Scientific Pages of the School of Civil Engineering, Nat. Tech. Univ. of Athens, Vol. 7, N° 2, 1983, pp. 17-31.*
- [5] J. Demetriou, Applied Hydraulics (Book Published by the National Technical University of Athens/Greece, 2008, pp. 184-187 and 229-241).
- [6] D. W. Knight and J. D. Demetriou, Flood Plain and Main Channel Flow Interaction, *Journal of Hydraulic Engineering, ASCE, Vol. 109, N° 8, 1983, pp. 1073-1092.*